Eur Biophys J
DOI 10.1007/s00249-015-1052-7

ORIGINAL PAPER

EBSA
Biophysics in Europe

Detailed study of the dielectric function of a lysozyme solution studied with molecular dynamics simulations

Stelios Floros[1] · Maria Liakopoulou-Kyriakides[1] · Kostas Karatasos[1] · Georgios E. Papadopoulos[2]

Received: 14 December 2014 / Revised: 28 May 2015 / Accepted: 2 June 2015

Abstract The spread of microwave technology and new microwave applications in medicine have revitalized interest in the dielectric behavior of biological systems. In this work, the Fröhlich–Kirkwood approach and the linear response theory have been applied in conjunction with molecular dynamics simulations to study the dielectric response of a lysozyme solution as a model. The overall experimental dielectric behavior of a 9.88 mM lysozyme solution has been reproduced in a quantitative manner by employing a method based on the decomposition of the hydration shells close to the solute. Detailed analysis of the calculated spectra identified two δ-processes located at 200 MHz (δ1) and about 1 GHz (δ2), respectively. δ1 is associated mainly with the first hydration shell, while δ2 mainly with bulk water and the second hydration shell. Moreover, indications for the existence of an even faster relaxation in the 10^{11}-Hz frequency range were found for the first time. Finally, the static dielectric constants of lysozyme and its first and second hydration shells were calculated based on the Fröhlich–Kirkwood and the linear response theory approaches.

Keywords Dielectric function · Protein · Hydration · Molecular dynamics simulations

Abbreviations

F–K	Fröhlich–Kirkwood
LRT	Linear response theory
MD simulations	Molecular dynamics simulations
2CD	2 Component decomposition
DD	Detailed decomposition
P	Protein
W	Water
S1	First hydration shell
S2	Second hydration shell
B	Bulk water
P and nP	Polar and nonpolar water molecules in the subsection "Decomposition of the first hydration shell"

Introduction

The study of dielectric relaxation in biological solutions is a task of great importance because it can offer useful information on the physicochemical properties of biomolecules. In the case of protein solutions, numerous relevant studies have been carried out for more than six decades (South and Grant 1972; Pethig 1992; Miura et al. 1994; Suzuki et al. 1996; Nandi and Bagchi 1998; Yokoyama et al. 2001; Knocks and Weingartner 2001; Hayashi et al. 2002; Cametti et al. 2011). These studies have revealed that the dielectric spectrum of such systems can be well described by three main relaxation mechanisms, the so-called β-, γ-, and δ-processes. The β-process reflects the overall tumbling of the protein and is located near the frequency of 10^7 Hz of the dispersion curve, while the γ-process can be rationalized by the reorientation of bulk water and is centered near 10^{10} Hz. Finally, the δ-relaxation process near 10^8–10^9 Hz is thought to arise from either the motions of protein-bound

✉ Georgios E. Papadopoulos
geopap@bio.uth.gr

[1] Department of Chemistry, Faculty of Chemical Engineering, Aristotle University of Thessaloniki, 54124 Thessaloniki, Greece

[2] Department of Biochemistry and Biotechnology, University of Thessaly, Ploutonos 26 and Aeolou, 41221 Larisa, Greece

Published online: 21 June 2015

water molecules or from motions of charged side chains of the proteins. Early dielectric spectroscopy experiments by Harvey and Hoekstra (1972) on hydrated powders of lysozyme assigned the two observed distinct dispersions to a first hydration shell with a relaxation time near 1 ns and to a second one near 0.02 ns. Moreover, the data suggested a lower degree of hydrogen bonding for the first hydration shell than in bulk water. As found by combining SAXS and SANS experiments on lysozyme solutions (Svergun et al. 1998), this partially immobilized water (first hydration shell) has a density about 10 % larger than the bulk and a thickness of 3 Å. MD simulations on ubiquitin and two other proteins (Rudas et al. 2006) found the structural and dynamic properties of water in a distance of $\leq$3.5 Å from the protein surface to be locally dependent on the physicochemical properties of the amino acid side chains in contact, distinct from those of bulk. According to the same work, the properties of the next hydration shell (between 3.5 and 6 Å) differ from those of bulk, but uniformly. THz spectroscopy on protein λ*6-85 accompanied with MD simulations (Ebbinghaus et al. 2007) extended the protein influence on the dynamic properties of surrounding water up to 10 Å. Although the δ-process contributes the least to the dispersion curve, in recent years it has been studied intensively in order to shed light in the protein–water interactions of the first hydration shell. These interactions may play a key role in the biological activity and functionality of proteins. Despite the large number of dielectric experimental studies, there is not yet a generally accepted molecular interpretation of the macroscopic findings. The main reason is that different relaxation mechanisms either partially or totally overlap in the relevant polarization regions of the spectrum. This is why molecular dynamic (MD) simulations (Nakamura et al. 1988; King et al. 1991; Simonson et al. 1991; Smith et al. 1993; Antosiewicz et al. 1994; Simonson and Perahia 1995; Yang et al. 1995; Loffler et al. 1997; Boresch et al. 1999, 2000) can play a crucial role as a useful tool to enhance our understanding of the dielectric properties of proteins. Usually, MD simulations apply the Fröhlich–Kirkwood (F–K) (Kirkwood 1939; Onsager 1936; Fröhlich 1958; Neumann et al. 1984; Neumann 1986a, b) and the linear response theory (LRT) (Kohler 1972; Neumann and Steinhauser 1983a, b; Neumann et al. 1984; Caillol et al. 1986, 1989; Loffler et al. 1997; Boresch et al. 2000; Weingärtner et al. 2001) in order to calculate the frequency-dependent dielectric constants. In the last decades, a large number of pioneering molecular simulation studies attested the feasibility of separating the individual contributions of a solution's components to the overall dielectric constant (Loffler et al. 1997; Boresch et al. 2000; Weingärtner et al. 2001). However, most of these studies failed to reproduce quantitatively the majority of experimental findings, including the value of the static dielectric constant of proteins, the position of the absorption peaks, and the δ-process. In this work, we apply the above-mentioned theories using data from molecular dynamics simulations and (a) demonstrate that these discrepancies can be largely diminished by employing sufficiently long simulation times and using a method of temperature control (Langevin thermostat), which is known to produce trajectories in the targeted statistical ensemble, and (b) we target the issue of the δ-process applying the shell decomposition method. Moreover, in sight of the importance of the electrostatic interactions in protein–protein interactions and protein folding, we calculated the static dielectric constant for lysozyme as well as for its first and second hydration shells.

Theoretical background

In this section, an outline of the basic theory for the calculation of the static and frequency-dependent dielectric constant of a solution is given. Further details can be found elsewhere (Simonson et al. 1991 and articles cited above).

The static dielectric constant of a material can be calculated by the following expression:

$$\varepsilon = \frac{\langle \mathbf{M}^2 \rangle - \langle \mathbf{M} \rangle^2}{3V\varepsilon_0 kT} + 1 \tag{1}$$

where **M** is the total dipole moment of the solute (lysozyme in this case), ε_0 is the permittivity of free space, V is the volume of protein assumed to be a sphere, k is Boltzman's constant and T is the temperature. The above formula results from the approach of F–K dielectric theory and has a form that is appropriate for dielectric calculations of systems under periodic boundary conditions (Yang et al. 1995; Boresch and Steinhauser 1997).

The overall frequency-dependent dielectric constant assuming a system of m components can be estimated by Eq. (2).

$$\varepsilon(\omega) - 1 = \frac{\chi(\omega)}{\varepsilon_0} = \frac{1}{\varepsilon_0} \sum_{i=1}^{m} \sum_{j=1}^{m} \chi_{ij}(\omega) \tag{2}$$

where $\varepsilon(\omega)$, $\chi(\omega)$ are the total dielectric constant and susceptibility of solution, while χ_{ij} is the pair susceptibility of components i, j. In turn, each of the pair susceptibilities can be expressed in terms of the so-called dipole–dipole auto- and cross-correlation functions via the following formula:

$$\chi_{ij}(\omega) = \frac{1}{3k_B VT} \mathrm{L}\left[-\frac{\mathrm{d}\Phi_{ij}(t)}{\mathrm{d}t} \right] \tag{3}$$

with

$$\Phi_{ij}(t) = \langle \mathbf{M}_i(t) \cdot \mathbf{M}_j(0) \rangle \tag{4}$$

where L denotes the Fourier–Laplace transform (Smith 1999). Here V is the volume of the simulation cell. Equation (3) is a result of the linear response theory. For a better optical comparison of the relaxation functions in Figs. 2, 5, and 7, we introduce the normalized $\Phi_{ij}(t)$, defined as:

$$\tilde{\Phi}_{ij}(t) = \frac{\langle \mathbf{M}_i(t) \cdot \mathbf{M}_j(0) \rangle}{\langle \mathbf{M}_i(0) \cdot \mathbf{M}_j(0) \rangle}$$

The calculation of $\Phi_{ij}(t)$ is based on the decomposition into auto ($i = j$) and cross ($i \neq j$) terms of the time varying dipole moments $\mathbf{M}(t)$ of the particular components. The dipole moment of component i at time step n of a molecular dynamics simulation trajectory is calculated by:

$$\mathbf{M}_{i,n} = \sum_{k=1}^{N} q_k \mathbf{r}_{k,n} \tag{5}$$

Here q_k is the partial charge of atom k and r_k the position vector of atom k. It is important to mention that in case of charged systems, their dipole moment depends on the choice of the origin of the coordinate system. The most appropriate choice for such systems is to take the dipole moment with respect to the mass center of the system (Loffler et al. 1997; Rudas et al. 2006).

For a system consisting of a protein, water, and ions according to Eq. (4), the total dipole moment correlation function can be written as:

$$\begin{aligned}\Phi_{\mathrm{tot}}(t) = {} & \Phi_{\mathrm{PP}}(t) + \Phi_{\mathrm{WW}}(t) + \Phi_{\mathrm{II}}(t) \\ & + 2\Phi_{\mathrm{PW}}(t) + 2\Phi_{\mathrm{PI}}(t) + 2\Phi_{\mathrm{WI}}(t)\end{aligned} \tag{6a}$$

where the subscripts P, W, and I stand for protein, water, and ions, respectively.

As shown in the Appendix, the relative contribution of $\Phi_{\mathrm{II}}(t)$ in $\Phi_{\mathrm{tot}}(t)$ is negligibly low and can be neglected. Inserting $\Phi_{\mathrm{PI}}(t)$ and $\Phi_{\mathrm{WI}}(t)$ in Eq. (3) yields expressions of $\langle \mathbf{M}_{\mathrm{P}}(t) \cdot \mathbf{J}_{\mathrm{I}}(0) \rangle$ and $\langle \mathbf{M}_{\mathrm{W}}(t) \cdot \mathbf{J}_{\mathrm{I}}(0) \rangle$, which according to our data (not shown) are practically null. Therefore $\Phi_{\mathrm{PI}}(t)$ and $\Phi_{\mathrm{WI}}(t)$ can also be neglected.

For a better resolution of the processes related to dipolar relaxation in dielectric experiments, the spectrum of dielectric loss is taken by subtracting the DC conductivity of ions ($i\sigma_0/\varepsilon_0\omega$). Otherwise, the regions of the β, γ and δ-processes may not be well resolved (Cametti et al. 2011). We also follow this convention in this work.

In addition, there are two different approaches at the studying of the dielectric phenomena. The usual two-component decomposition (2CD, protein–water) approach suggests that the cross term Φ_{PW} contributes in the description of the δ-relaxation process and must be considered. On the other hand, according to a detailed decomposition (DD) approach (Rudas et al. 2006), correlations of a more detailed system decomposition should be taken into account for the spectral identification of the different contributions in the region of the δ-process. In this context, the water relaxation Φ_{WW} is separated into auto-correlations of the first hydration shell (Φ_{S1S1}), of the second hydration shell (Φ_{S2S2}), of the bulk water (Φ_{BB}) and of cross-correlations of the two shells with bulk water, (Φ_{S1B}) and (Φ_{S2B}), as well as between the two shells (Φ_{S1S2}).

According to the above considerations, the total relaxation of the system will be described for the 2CD approach by:

$$\Phi_{\mathrm{tot}}(t) = \Phi_{\mathrm{PP}}(t) + \Phi_{\mathrm{WW}}(t) + 2\Phi_{\mathrm{PW}}(t) \tag{6b}$$

and for the DD one by:

$$\begin{aligned}\Phi_{\mathrm{tot}}(t) = {} & \Phi_{\mathrm{PP}}(t) + \Phi_{S1S1}(t) + \Phi_{S2S2}(t) + 2\Phi_{S1S2}(t) \\ & + 2\Phi_{S1B}(t) + 2\Phi_{S2B}(t) + \Phi_{BB}(t)\end{aligned} \tag{6c}$$

The term $\Phi_{\mathrm{PW}}(t)$ was not taken into account in Eq. (6c) due to its large fluctuations, which lead to low-quality fits and therefore to a not well interpretable δ-region.

Based on the expected dynamic behavior, each normalized term of Eq. (6b) can be determined by fitting the data for each contribution with a sum of exponential functions. A bi-exponential fit (Eq. 7a) was found sufficient for this purpose:

$$\tilde{\Phi}(t) = A_1 \exp(-t/\tau_1) + A_2 \exp(-t/\tau_2) \tag{7a}$$

Estimates of the fit quality can be given using E_{rms} and R^2 for non-linear least square fitting:

$$E_{\mathrm{rms}} = \sqrt{\frac{\sum_1^N [C_n - \Phi_n]^2}{N-4}},\ R^2 = 1 - \sum_1^N (C_n - \Phi_n)^2 / \sum_1^N \left(C_n - \hat{C}_n\right)^2 \tag{7b}$$

In Eq. (7b), C_n is the value of the calculated correlation function at lag time step n, Φ_n is its fitted value at the same lag time step and $\hat{C}_n$ is the average value of C_n. N is the total number of lag time steps.

Function $\tilde{\Phi}(t)$ (Eq. 7a) in the frequency domain corresponds to two Debye processes characterized by their amplitudes (A_1, A_2) and their relaxation times (τ_1, τ_2). It is not possible to relate these amplitudes alone to the amount of the material that contributes to the process, as its total dipole moment depends on both the number of dipoles and on their polarizations. A small number of polarized dipoles may exhibit a greater total dipole moment than that of a large number of dipoles but with stochastic orientations. If these distinct relaxations should be attributed to different groups of molecules of the same kind but with different dielectric behavior, one could express their $\Phi(t)$ as a sum of their auto- and cross- correlation functions. However, it cannot be excluded that an individual water molecule can contribute to several relaxation processes depending on its momentary interactions with its neighbors (e.g., via hydrogen bonds) without assuming a grouping in different space partitions. The definition of A_i and τ_i leads to the

final expressions for the real and imaginary part of the frequency-dependent dielectric constants:

$$\mathrm{Re}\ \varepsilon(\omega) = \sum_{i=1}^{m} B_i \left(1 - \frac{A_{i1}\tau_{i1}^2\omega^2}{1+\omega^2\tau_{i1}^2} - \frac{A_{i2}\tau_{i2}^2\omega^2}{1+\omega^2\tau_{i2}^2} \right) \tag{8a}$$

$$\mathrm{Im}\ \varepsilon(\omega) = \sum_{i=1}^{m} B_i \left(\frac{A_{i1}\tau_{i1}\omega}{1+\omega^2\tau_{i1}^2} + \frac{A_{i2}\tau_{i2}\omega}{1+\omega^2\tau_{i2}^2} \right) \tag{8b}$$

with

$$B_i = \frac{\langle \mathbf{M}_i(0) \cdot \mathbf{M}_i(0) \rangle}{3\varepsilon_0 k_B V T} \tag{9}$$

Here, i stands for PP, WW, and PW.

For the terms S1S1, S2S2 of Eq. (6c), a tri-exponential fit is found to be more appropriate, leading to the following final equations:

$$\mathrm{Re}[\varepsilon(\omega)] = \sum_{i=1}^{m} B_i \left(1 - \frac{A_{i1}\tau_{i1}^2\omega^2}{1+\omega^2\tau_{i1}^2} - \frac{A_{i2}\tau_{i2}^2\omega^2}{1+\omega^2\tau_{i2}^2} - \frac{A_{i3}\tau_{i3}^2\omega^2}{1+\omega^2\tau_{i3}^2} \right) \tag{10a}$$

$$\mathrm{Im}[\varepsilon(\omega)] = \sum_{i=1}^{m} B_i \left(\frac{A_{i1}\tau_{i1}\omega}{1+\omega^2\tau_{i1}^2} + \frac{A_{i2}\tau_{i2}\omega}{1+\omega^2\tau_{i2}^2} + \frac{A_{i3}\tau_{i3}\omega}{1+\omega^2\tau_{i3}^2} \right) \tag{10b}$$

Simulation details

The initial structure of lysozyme was obtained from the Protein Data Bank (PDB entry: 2LZT) and has been solvated in an orthogonal box ($48.10 \times 52.40 \times 66.65$ Å^3) with 4672 TIP3P water molecules resulting in a protein concentration of 9.88 mM ($w/w = 14.5$ %, mass of H_2O over dry protein = 5.88). The adopted concentration is a compromise between computational affordability and the value used in dielectric experiments (Cametti et al. 2011). Disulphide bonds have been added at Cys6-Cys27, Cys30-Cys115, Cys64-Cys80, and Cys76-Cys94. The positive charge of lysozyme (+8) has been neutralized by the addition of ions (18 Na^+ and 26 Cl^-). The molecular dynamics program NAMD (Kale et al. 1999) and the CHARMM force field (Brooks et al. 1983) have been employed to minimize energy and pre-equilibrate the system for 2.5 ns followed by a production run of 30 ns with Langevin thermostat ($\gamma = 5$/ps) at 300 K in the NVT ensemble. Additionally, 30 independent 2.5-ns simulations have been performed (starting from the well-equilibrated system of the previous 30-ns simulation) to improve the statistics for the calculation of the dielectric properties of the water component. The SHAKE algorithm (Ryckaert et al. 1977) has been applied to all bonds and interactions were calculated within a range cut-off radius of 16 Å. Electrostatic interactions were calculated with the particle Mesh Ewald technique (Darden et al. 1993) while assuming tin-foil boundary conditions. The time step of the simulations was 2 fs, and configurations of the long-time simulation system were stored every 0.5 ps, while for the short-time simulations every 0.06 ps. In order to isolate a hypothetical effect of protein on water's dielectric behavior, an additional series of four 2.5-ns simulations has been carried out of a system containing only water and ions. Each water box contained 4672 water molecules (the same as before) and ions (21 Na^+ and 21 Cl^-). All other simulation parameters were exactly the same as those of the short-time simulations. One 800-ps simulation with frames saved every one 1 fs has been performed in order to study the contribution of ions (including protein) in the overall dielectric spectrum.

The simulation data have been analyzed using custom-made Tcl scripts running via the VMD program (Humphrey et al. 1996). Furthermore, the gnuplot program has been used for fitting of the correlation curves. The volume for each subregion was calculated using the program MSMS (Sanner et al. 1996) as an average over the trajectory of the long simulation.

Results and discussion

The findings about the ion contribution are presented in the Appendix.

Dielectric analysis according to the 2CD approach

In this subsection, the trajectory of a 30-ns NVT simulation of the already-equilibrated (NPT) system is being analyzed in the frame of the 2CD approach (Eq. 6b). Only the last 13.5 ns of this simulation were used for trajectory analysis, since at this time interval the fluctuations of the dipole moment of the lysozyme converge to a static plateau. According to our experience, the convergence of the protein's dipole moment fluctuations is a necessary condition for the proper estimation of Φ_{PW}. The dipole moment fluctuations per volume versus simulation time of the protein are shown in Fig. 1, where we observe that after 10 ns, the fluctuations reach a static value of about 178.

Figure 2 shows the normalized auto- and cross-correlation functions of the systems components according to the 2CD (PP, PW, and WW) as calculated from the simulation data, as well as their corresponding fits.

As it is obvious from Fig. 2, $\tilde{\Phi}_{\mathrm{PP}}$ and $\tilde{\Phi}_{\mathrm{WW}}$ show the expected relaxation behavior with small fluctuations and allow reliable bi-exponential fits. On the other hand, $\tilde{\Phi}_{\mathrm{PW}}$ shows large fluctuations, which reduce the quality of the fit. Besides, $\tilde{\Phi}_{\mathrm{PW}}$ in our case contributes less than 4.5 %. For

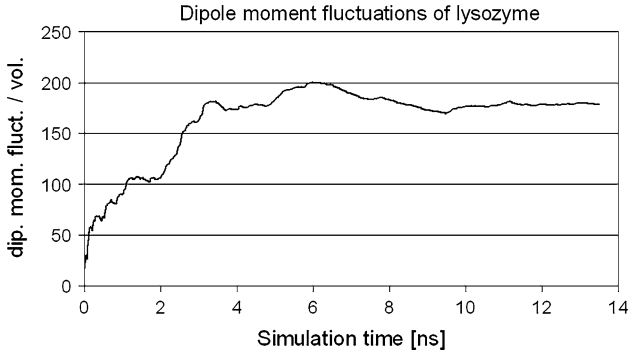

Fig. 1 Total dipole moment fluctuations of lysozyme per volume vs. simulation time. The last 13.5 ns of the 30-ns simulation has been used for this calculation

this reason, some theorists neglect the cross correlation in their calculations (Loffler et al. 1997; Boresch et al. 2000). Nevertheless, in our case, the quality of the plot is marginally good enough in order to fit it by an analytic bi-exponential function. The parameters of the corresponding fits are presented in Table 1.

According to Table 1, the PP auto-correlation function can be described with two relaxation processes, a very slow ($\tau_1 = 19035$ ps) dominant one ($A_1 = 0.956$) corresponding to the overall tumbling of protein, which is known as the β-process in a typical dielectric dispersion curve, and a faster one ($\tau_2 = 48$ ps) with a small contribution ($A_2 = 0.044$). It is worth mentioning that the above value of τ_1 is very close to that found experimentally (Bonincontro et al. 2001). The fast relaxation is assumed to originate from flexible parts of the protein and contributes in the spectrum with a small peak at 3.3×10^9 Hz as part of the δ-process (Fig. 3).

Another part of the δ-process is frequently attributed to the PW cross-correlation. This correlation is represented here by two relaxation processes. The fast relaxation with $\tau_2 = 55$ ps, with a spectral maximum located at 2.9×10^9 Hz, probably quantifies a combined loss of correlation between protein's dipole components (flexible and rigid parts) and the fast water component mostly from the bulk molecules with the highest rotational freedom. On the other hand, the more dominant ($A_1 > A_2$) slow relaxation ($\tau_1 = 7587$ ps) with a peak centered at 2.14×10^7 Hz may arise from the portion of water molecules that are tightly bound to the protein surface, as their total dipole moment needs longer time to become statistically independent from that of protein. However, considering the rather large fluctuations of the PW cross-correlation and the relatively high E_{rms} value of the fit as well as the low value of R^2, a clear assignment regarding the origin of the PW component is not possible.

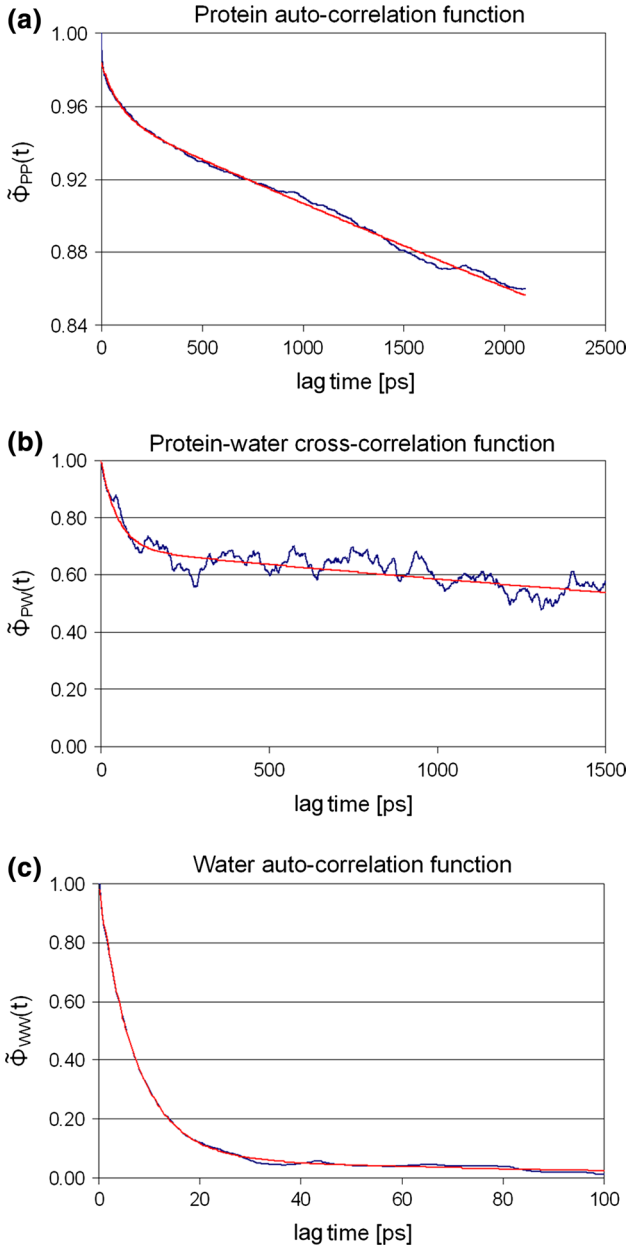

Fig. 2 Normalized auto- and cross-correlation functions as calculated from the simulation data (*blue lines*), as well as their corresponding fits (*red lines*). **a** Protein auto-correlation, **b** protein–water cross-correlation, and **c** water auto-correlation of a lysozyme solution (141.5 mg/ml) at 300 K

The WW relaxation is fully characterized by two relaxation processes, a dominant ($A_2 = 0.94$) fast one ($\tau_2 = 7.3$ ps) and a slower ($\tau_1 = 196$ ps) very weak in amplitude ($A_1 = 0.06$) process. The fast relaxation is consistent with freely rotating water molecules that characterize the bulk and gives rise to a large peak in the absorption spectrum at 2×10^{10} Hz, known as the γ-process (Fig. 4b). This relaxation time is very close to the experimentally observed value of 8.4 ps (Oleinikova et al. 2004) and 9.3 ps (Loffler et al.

Table 1 Parameters of exponential fits of the dipole moment auto- and cross-correlations and centers of the corresponding loss peaks for the two-component system (protein and water) at 300 K

	PP	PW	WW
A_1	0.956	0.687	0.06
τ_1 (ps)	19035	7588	196
f_1 (Hz)	1×10^7	2.14×10^7	1×10^9
A_2	0.044	0.313	0.94
τ_2 (ps)	48	55	7.3
f_2 (Hz)	3.3×10^9	2.9×10^9	2×10^{10}
$*E_{rms}$	0.002	0.049	0.005
R^2	0.9936	0.6683	0.9964

* E_{rms} and R^2 are calculated according to Eq. (7b)

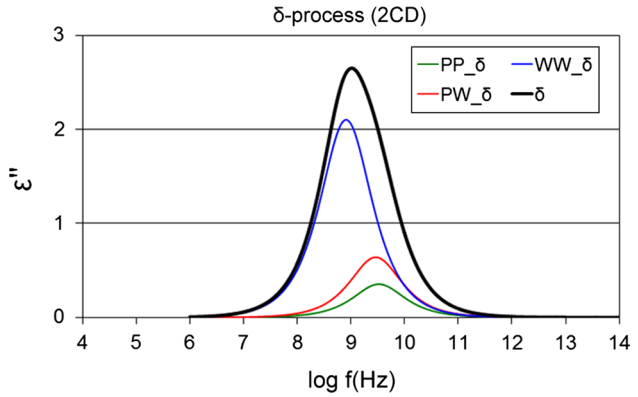

Fig. 3 The 2CD approach results in a rather monomodal δ-process (*black thick line*) located at ~10^9 Hz as a sum of the slow WW relaxation and the fast components of the PP (*green*) and PW (*red*) relaxations

1997). The slow relaxation contributes to the δ-process with a peak at 10^9 Hz (Fig. 3). In general, this process may arise from different contributions, such as from a portion of water molecules near the protein with less rotational freedom, from momentary restricted rotational motion of water molecules homogeneously distributed, or even from water molecules interacting with ions. The later can be safely excluded according to the results of our simulation on a system comprised solely of water and ions. Analysis of this simulation shows only one relaxation time ($\tau = 7.2$ ps) identical to that of the dominant relaxation of the 2CD system (Table 1). Another possibility could be the presence of some relatively long-living clusters of water molecules that may rotate as a whole. However, such a dielectric contribution has not been found, probably because highly spherically symmetric clusters may well assume vanishing total dipole moments. In order to shed light on this, a detailed study of the water surrounding the protein will be presented in the next section based on its decomposition.

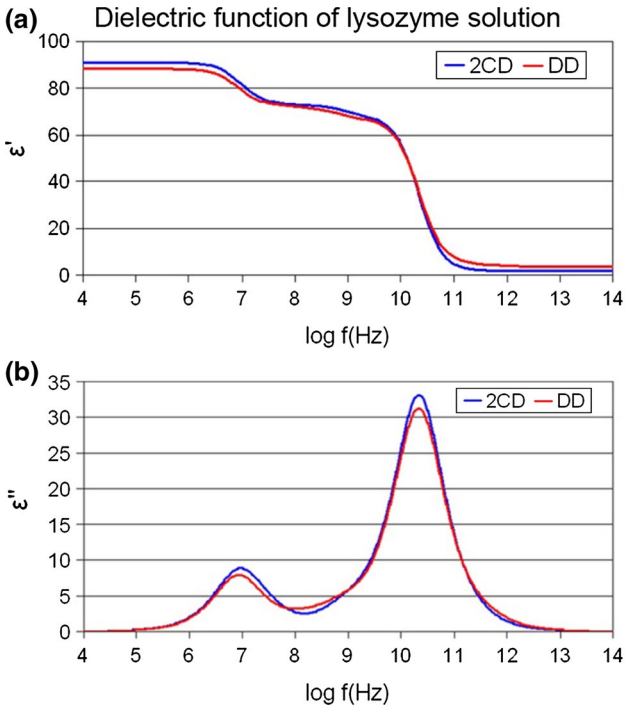

Fig. 4 Real (**a**) and imaginary (**b**) part of the dielectric function of a lysozyme aqueous solution ($C = 141.5$ mg/ml) as a function of frequency at 300 K. *Red line* according to the DD approach, *blue line* according to the 2CD approach (the slow part of PW is excluded due to its statistical poorness)

According to the above analysis (excluding the less reliable PW contribution), the δ-process is represented by a maximum at 1.9×10^9 Hz composed of two closely located peaks at 3.3×10^9 and 10^9 Hz near the δ2-process, as found experimentally (Cametti et al. 2011) (4×10^9 Hz) for concentrations above 50 mg/ml. It can be attributed mainly to the slow relaxation process of the water component and secondary to the fast relaxation of the protein. The relation between the expected δ1-process and the slow part of the PW correlation cannot be safely described due to the higher statistical error of the associated fit (Table 1).

Dielectric analysis according to the DD approach

Decomposition of the water contribution

In this approach, the water content of the simulation box has been divided into three parts, each one containing a certain population of water molecules. The first part contains those water molecules that have at least one atom located within 3 Å from the protein's surface and is taken here as the first hydration shell denoted by S1. Similarly, the second hydration shell (S2) contains water molecules within 6 Å from the protein's surface excluding those of S1. Water

molecules located at a distance greater than 6 Å from the protein's surface is characterized here as bulk (B). The above partitioning maximized the quantity $|\tau_1(S1)-\tau_1(S2)|$, where $\tau_1(S1)$ and $\tau_1(S2)$ are slow dipole moment auto-correlation relaxation times of S1 and S2, respectively. In the case of a collection of water molecules, the time lag needed for the dipole correlation function to de-correlate (i.e., approach a value close to zero) is practically no longer than ~100 ps. For this reason, a relatively short simulation (2–3 ns) is sufficient for the proper calculation of dipole correlation functions and also for the convergence of the dipole moment fluctuations to a plateau (especially for the calculation of the static dielectric constant). On the other hand, the number of water molecules in S1 and S2 is small compared to that in B, which leads to poor statistics and large fluctuations of the relaxation curves. In order to tackle this issue, the final exponential fit is performed on a dipole correlation curve resulting as an average of 30 correlation functions derived from equal in number independent 2.5-ns simulations (Fig. 5).

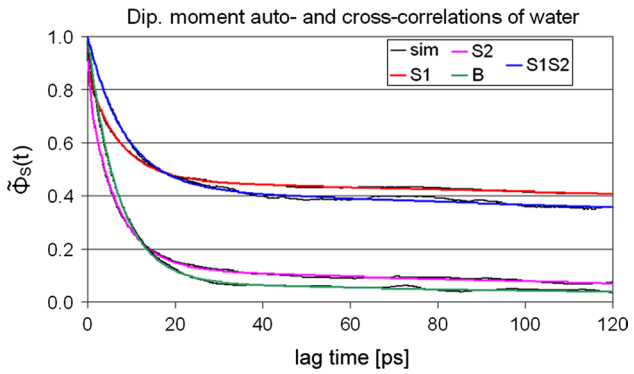

Fig. 5 Normalized dipole auto- and cross-correlation functions of hydration shells S1, S2, and of the bulk B of a lysozyme solution ($C = 141.5$ mg/ml) at 300 K. *Color lines* are fits to their corresponding simulation data (*black lines*)

In Fig. 5, the dipole moment auto- and cross-correlation functions of the various water partitions as well as their corresponding fit functions are plotted. The target functions of S1 and S2 auto-correlations were best described by three exponentials, while the cross-correlation data of S1S2 and the auto-correlation of B were best represented by bi-exponential fits. For the sake of clarity, the S1B and S2B cross-correlations are not shown in Fig. 5. All fit parameters are reported in Table 2.

As can be seen from Table 2, all water correlation functions show a similar fast relaxation (6.5 ps $< \tau_2 <$ 14.2 ps) in good agreement with literature (Neumann 1986a, b; Yang et al. 1995; Loffler et al. 1997; Oleinikova et al. 2007). This fast relaxation is very dominant in the case of the BB auto-correlation ($A_2 = 0.917$). It is exactly what is expected comparing with the corresponding τ_2 from WW of Table 1 and can be attributed to freely rotating water molecules. This is a rather reasonable assumption for bulk water molecules, but somewhat surprisingly for water molecules of the first and less surprising for those of the second hydration shell. However, water molecules hydrogen bonded to backbone carbonyls may be restricted in their rotations around axes perpendicular to the hydrogen bonds, but they could be almost free to rotate around their hydrogen bonds contributing to a change of the net dipole moment. All the above τ_2 contributions are combined giving rise to the γ-process at $\approx 2 \times 10^{10}$ Hz (Fig. 4b).

Another striking similarity concerns the slow relaxation component of S2S2 and BB. Both show a $\tau_1 \approx 195$ ps, which is reasonable for S2, as it may manifest the effect of the protein on the polarization dynamics of this part of the water molecules, but it is rather unexpected (even as a very small contribution) for water molecules in the bulk. The same value is also obtained in the frame of 2CD analysis (Table 1). This relaxation is the origin for a peak at 10^9 Hz (Fig. 6, δ2-process). The similarity in τ_1 between S2 and B reveals common dynamic processes taking place in both

Table 2 Parameters of exponential fits of the dipole moment auto- and cross-correlation data and centers of the corresponding loss peaks for the first two hydration shells as well as for the bulk water

	S1S1	S1S2	S1B	S2S2	S2B	BB
A_1	0.466	0.426	−0.417	0.13	−0.169	0.083
τ_1 (ps)	1106	663	48.5	195	89.8	194
f_1 (Hz)	1.48×10^8	2.3×10^8	3.31×10^9	1.0×10^9	1.74×10^9	1.0×10^9
A_2	0.395	0.574	1.147	0.675	1.169	0.917
τ_2 (ps)	7.3	8.5	14.2	6.5	10.4	6.8
f_2 (Hz)	2.16×10^{10}	1.8×10^{10}	1.1×10^{10}	2.4×10^{10}	1.5×10^{10}	2.2×10^{10}
A_3	0.139	–	–	0.194	–	–
τ_3 (ps)	0.3	–	–	0.4	–	–
f_3 (Hz)	5.7×10^{11}	–	–	4.1×10^{11}	–	–
$^*E_{rms}$	0.004	0.008	0.021	0.005	0.01	0.006
R^2	0.9978	0.9964	0.9254	0.9983	0.9961	0.9985

* E_{rms} and R^2 are calculated according to Eq. (7b)

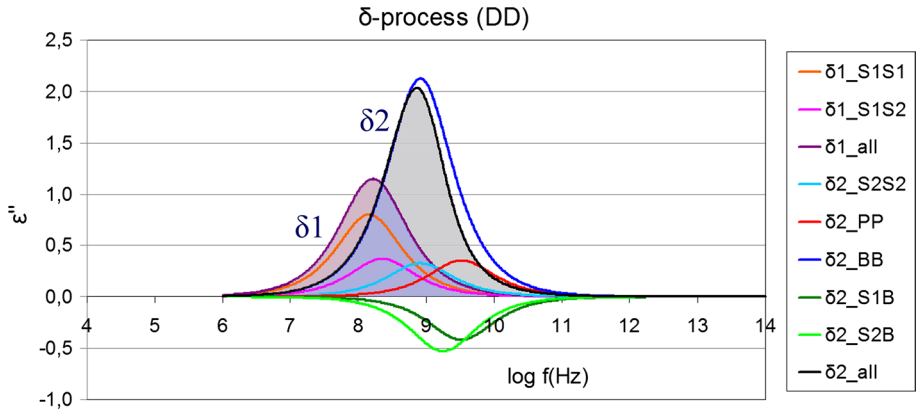

Fig. 6 The DD approach results in a bimodal δ-process (*filled curves*). The main contribution in δ1 comes from the slow S1S1 component, while that in δ2 from the slow BB one. The slow components of the cross terms S1B and S2B contribute negatively in δ2

water components but with very different probability. The cross-correlation S1S2 shows even larger τ_1 with an intermediate value of 663 ps, between the corresponding auto-correlations. This relaxation contributes to the δ-process at 2.3×10^8 Hz. The S1S1 auto-correlation besides the aforementioned fast component τ_2 also reveals a significant ($A_1 = 0.466$) slow component with $\tau_1 = 1106$ ps, which gives rise to a peak at 1.48×10^8 Hz. This slow de-correlation of the total dipole of S1 can be seen as a manifestation of the presence of almost immobilized water molecules in close contact with protein atoms bearing limited little rotational freedom. They could probably reside either near polar residues forming hydrogen bonds with them or deeper in protein clefts and near to accessible parts of protein's backbone. The decline in slow relaxation times [$\tau_1(S1) > \tau_1(S2)$, $A_1(S1) > A_1(S2)$] suggests a blanking-out effect of protein on water, extending beyond 6 Å from the protein's surface. The slow components of S1S1 and S1S2 give rise to two peaks at 1.48×10^8 and 2.3×10^8 Hz, which combine to form a peak at 2×10^8 Hz. This frequency is very close to that of the δ1-process found spectroscopically (Cametti et al. 2011) at 10^8 Hz. On the other hand, the synthesis of the slow component of S1B, S2B, S2S2, and BB with the fast component of PP make the δ2-process, which in our case is peaked near 10^9 Hz somewhat lower than the experimental value of 4×10^9 Hz (Cametti et al. 2011). The negative ε'' peaks originated from the slow S1B and S2B cross terms signify anticorrelations between S1, S2, and the bulk water. Similar findings regarding S1B (not S2B) have been reported by Rudas et al. (2006) for 1ubq and 1clb. Notice that S1B and PP almost cancel out. The above-described contributions explain sufficiently the experimentally found δ1 and δ2 processes (Fig. 6). At first glance, the location as well the height of the δ2 peak seem to be in disagreement with those reported by Cametti et al. (2011). However, Cametti et al. suggest a shift of δ2 to lower frequencies and higher ε'' values with protein concentration. Consequently, this difference can be attributed to the high concentration (141.5 mg/ml) of our system.

The last paragraph of this section focuses on the third very fast (0.3 and 0.4 ps) relaxation present in the S1 and S2 autocorrelation functions, which is not straightforward to interpret, but it cannot be ignored as it shows a not insignificant contribution in the total auto-correlation function (0.14 and 0.19, respectively). If it is not a result of our methodological artifacts, it deserves more attention from experimentalists. The identification of this fast relaxation was possible due to a 0.06 ps recording of frames in the MD trajectory. This fast relaxation could be attributed to water molecules in the immediate vicinity of the protein, which do not share hydrogen bonding with other water molecules. This is reasonable near polar protein residues, while near non-polar residues it would be less probable. We recall here that we consider auto- and cross-correlations of the net dipole moment of collections of water molecules. Therefore, fluctuations of the net dipole moment can also arise from combinations of principal rotations (librations) of water molecules around axes not along their dipole moments. These rotations may be actually even faster than in bulk, because of the absence of an extended inter-water network, and are similar to those observed by classical and QM/MM MD simulations for water in aqueous Ni(II) solution (Inada et al. 2002). In contrary, in the case of bulk water, and because of its isotropic character, such very fast local charge redistributions rather cancel out, unable to produce net dipole fluctuations. In a lack of available experimental or prior protein–water simulation data related to a so fast de-correlation of the dipole moment, we will refer to the process at $\approx 5 \times 10^{11}$ Hz as "ε-process." Although detectable in simulation because of the detailed analysis afforded by this method, experimental verification of the ε-process could be a tedious task which would require experimental apparatus that could operate reliably at frequencies exceeding 10^{11} Hz and noise-free data that would render possible its resolution near (or even overlapping with) the dominant γ-process at this frequency range.

In the next section, we attempt to interpret the basic characteristics of the S1 shell after decomposing it in polar (P) and non-polar (nP) water molecules.

Decomposition of the first hydration shell

In this section, a more detailed dielectric study of the S1 shell will be attempted by grouping its water molecules into two populations according to their neighboring to polar or non-polar residues. Water molecules of the S1 shell whose distance to polar residues is shorter than that to non-polar are categorized as polar (P, not to be confused with the notation for protein as in the 2CD approach) while the rest as non-polar (nP).

The above definitions lead to three contributions in the S1S1 auto-correlation function (Eq. 11), and each of them may be mono-, bi-, or tri-exponential.

$$\langle \mathbf{M}_{S1}(0) \cdot \mathbf{M}_{S1}(t) \rangle = \langle \mathbf{M}_{P}(0) \cdot \mathbf{M}_{P}(t) \rangle + \langle \mathbf{M}_{nP}(0) \cdot \mathbf{M}_{nP}(t) \rangle + 2\langle \mathbf{M}_{P}(0) \cdot \mathbf{M}_{nP}(t) \rangle \quad (11)$$

The fit-parameters for each of the contributions of Eq. (11) are depicted in Table 3 and their corresponding relaxations are plotted in Fig. 7. It is obvious from the parameters of Table 3 that the cross-term provides the slowest (1557 ps) dielectric relaxation process of the first hydration shell. As expected, polar and non-polar water molecules of S1 differ in their τ_1 values, with polar waters bearing larger τ_1 than non-polar ones, but the difference is surprisingly low. The decomposition of S1 provided for each subgroup almost the same relaxation picture as in Table 2 and did not result in mono-exponential relaxations. Both groups also share bulk dielectric properties.

Considering the two analyzed approaches (2CD and DD), we conclude that the DD not only represents better the overall dielectric behavior of a lysozyme solution but it also offers a more detailed picture of the studied system. It is worth noting that the inability of the 2CD approach to correctly describe the dielectric behavior of the biological water is based on the failure of the fitting procedure to detect a slow relaxation time from the WW relaxation found in the S1 water shell. This is due to the very small number of S1 water molecules relative to the rest whose properties dominate over S1. A slow relaxation could presumably be detected also through the PW relaxation had the fluctuations been smaller in order to allow a reliable analysis of the spectra.

Employing MD simulations, Soda et al. (2011) studied the water populations of lysozyme's hydration sites and classified them as external or internal, and additionally subdivided into clustered or single. The major external clustered hydration site hosts about six bridging water molecules, each being hydrogen bonded to more than one protein polar group, and is located in the substrate binding cleft. Following the notation of Soda et al. (2011), we refer to this site as Clft. The most populated external single hydration site is notated by S, and hosts on average 0.37 water molecules. On the other hand, the major internal hydration site is notated by Hg and accommodates on average 4.8 water molecules. The above sites consist of backbone and side-chain polar groups [see Soda et al. (2011) for details].

Water molecules belonging to these hydration sites are structurally and functionally important, and therefore it is interesting to calculate their dielectric properties. Analysis of 30 independent MD trajectories resulted in dipole moment autocorrelation functions and in the corresponding relaxation times and frequencies shown in Fig. 8 and Table 4, respectively.

Each of the three relaxations in Fig. 8 can be very well represented by a tri-exponential fit. The slow relaxation

Table 3 Parameters of exponential fits of the normalized dipole moment auto- and cross-correlations and centers of the corresponding loss peaks for polar and non-polar water molecules of S1

	P	nP	PnP
A_1	0.4	0.3	0.7
τ_1 (ps)	979.7	874.7	1557.4
f_1 (Hz)	1.62×10^8	1.82×10^8	1.01×10^8
A_2	0.4	0.4	0.3
τ_2 (ps)	6.53	6.44	10.67
f_2 (Hz)	2.44×10^{10}	2.46×10^{10}	1.49×10^{10}
A_3	0.2	0.3	–
τ_3 (ps)	0.26	0.16	–
f_3 (Hz)	6.16×10^{11}	1.05×10^{12}	–
E_{rms}	0.004	0.005	0.007
R^2	0.9968	0.9957	0.9839

* E_{rms} and R^2 are calculated according to Eq. (7b)

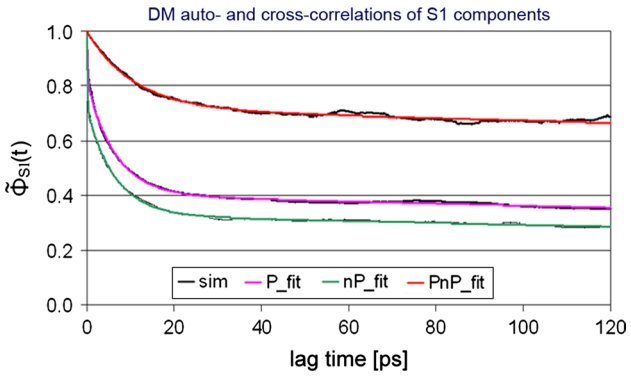

Fig. 7 Normalized dipole auto- and cross-correlation functions of hydration shell S1 components (P, nP, PnP). *Color lines* are fits to their corresponding simulation data (*black lines*)

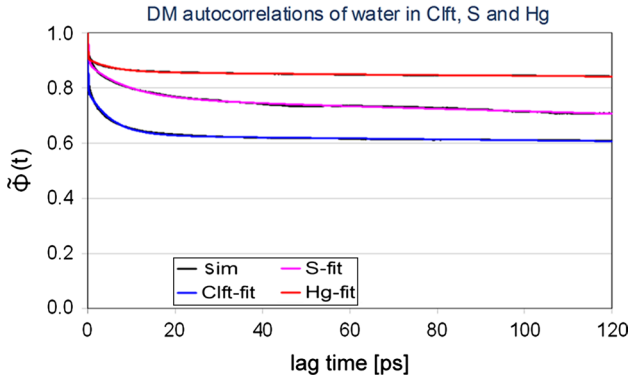

Fig. 8 Normalized dipole auto-correlation functions of water in hydration sites Clft, S and Hg. *Color lines* are fits to their corresponding simulation data (*black lines*)

Table 4 Parameters of exponential fits of the normalized dipole moment auto-correlations and centers of the corresponding loss peaks for water molecules belonging to major clustered or single hydration sites

	Clft	S	Hg
A_1	0.63	0.76	0.86
τ_1 (ps)	3564.9	1571.3	6315.1
f_1 (Hz)	4.5×10^7	1.0×10^8	2.5×10^7
A_2	0.16	0.13	0.05
τ_2 (ps)	5.32	9.09	5.53
f_2 (Hz)	3.0×10^{10}	1.7×10^{10}	2.9×10^{10}
A_3	0.21	0.11	0.09
τ_3 (ps)	0.08	0.24	0.08
f_3 (Hz)	1.9×10^{12}	6.4×10^{11}	1.9×10^{12}
E_{rms}	0.004	0.005	0.007
R^2	0.9968	0.9957	0.9839

* E_{rms} and R^2 are calculated according to Eq. (7b)

component of water molecules in the selected hydration sites is in all three cases dominant (Table 4), reflecting relatively long-living orientations of water molecules hydrogen bonded to protein polar groups. Bridging water molecules of the Clft clustered sites with $\tau_1 = 3564.9$ ps and hidden water molecules of the Hg site with $\tau_1 = 6315.1$ ps, which form a compact internal network, are expected to have very small orientational and translational freedom and to show slow components in the same order of magnitude as those of the PW relaxation (Table 1). Probably, these water molecules as well as others from similar hydration sites follow partially the breathing motion of the protein backbone and can account for the slow component of the PW relaxation. Water reorientation can happen when hydrogen bonds are destabilized due to thermal fluctuations in the related atom positions. Fluctuations of internal groups are of smaller amplitude compared to those of external ones, and this leads to a smaller rate of reorientations of water trapped in the compact protein interior.

In the case of hydration site S, and in order to achieve better statistics, we relaxed the angle criteria for hydrogen bonding in selecting the relevant water molecules. This together with the fact that external side chain polar groups are more mobile than backbone ones can explain why S site water exhibits a faster slow component ($\tau_1 = 1571.3$ ps) than Clft and Hg comparable to those of S1S1 (Table 2), P and PnP (Table 3) relaxations. The differences in the relative contributions between S and S1 expressed in A_1 reflect the fact that the first hydration shell also includes water molecules not hydrogen-bonded to the protein. The slow component of water molecules in Clft, S, and Hg are the main contributors to the δ1-process.

Besides their very slow component, all the above groups also show a less contributing characteristic relaxation time of bulk water of ~7 ps found in S1 and S2 too. The ultra-fast reorientations giving rise to the ε-process are still present in all three hydration sites. Interestingly enough, water molecules in the Clft and Hg cluster sites give fast relaxation times of 0.08 ps, i.e., faster than that of S waters ($\tau_3 = 0.24$ ps).

Static dielectric constant

In this section, the static dielectric constants of lysozyme and of its hydration shells S1 and S2 are calculated resulting from two different formalisms, according to Eq. (1) (F–K) and Eq. (2) (LRT), respectively. The F–K formalism is valid for homogeneous systems with spherical symmetry, which is an oversimplifying assumption for a protein. The static dielectric constant of the S1 shell can be calculated using Eq. (1) as the difference between the system containing the protein and S1 and that of the protein. The static dielectric constant for the S2 shell can be calculated in a similar way. The alternative for the calculation of the static dielectric constants is the LRT formalism at the low frequency limit ($\omega \to 0$), taking into account all dipole moment auto- and cross-correlations. The values of the so-calculated static dielectric constants, their percent difference, as well as the average volumes of the subsystems, are given in Table 5.

As is obvious from Table 5, both formalisms give almost the same value for the static dielectric constant of lysozyme, 18.8 and 18.3, respectively, with a difference of 2.7 %. These values are very close to the value of 15 derived from dielectric experiments by Harvey and Hoekstra (1972) in powders of lysozyme. Also in the case of S1, both formalisms lead to very close to each other's values (7.1 and 6.7, respectively) with a 5.4 % difference. However, in case of the S2 shell, the two constants (14.0 and 11.0, respectively) differ significantly from each other (24 %). The reason for this discrepancy is probably the breakdown of the assumption for homogeneity (protein + water) for the validity of

Table 5 Static dielectric constants and average volumes of lysozyme, S1, and S2 hydration shells

	ε[a]	$\varepsilon\ (\omega \to 0)$[b]	Difference (%)	V (nm^3)
Lysozyme	18.8	18.3	2.7	17.35
S1	7.1	6.7	5.8	11.81
S2	14.0	11.0	24.0	18.97

[a] Calculation according to F–K formalism

[b] Calculation according to LRT at the low frequency limit

Eq. (1). To our knowledge, there are no values from the literature for the static dielectric constant of S2. Caution is required when comparing values derived from experimental data at different conditions, because the dielectric constant depends on both temperature and protein concentration.

Conclusions

In this work, a series of molecular dynamic simulations were performed in order to study the dielectric properties of a lysozyme solution (141.5 mg/ml) at 300 K. According to experimental studies mentioned in the Introduction, protein solutions have a common dielectric behavior, where the imaginary part of $\varepsilon(\omega)$ displays two peaks, a more prominent near 2×10^{10} Hz (γ-process) corresponding to the absorption of water and a weaker one centered at 10^7 Hz (β-process) corresponding to the absorption of protein. Concerning these spectral features, our dielectric spectra of the lysozyme solution are in perfect qualitative as well as quantitative agreement with most of the experimental results. However, there is no general agreement for the location and interpretation of the δ-process, which is located in the range of 10^8–3×10^9 Hz, and whose dielectric behavior puzzles experimentalists as well as theoreticians. We followed a hydration shell decomposition approach and have demonstrated that the δ-process is bimodal with $\delta 1$ centered at 2×10^8 Hz (close to 10^8 found experimentally) and $\delta 2$ at about 10^9 Hz deviating somewhat from the experimental value of 4×10^9 Hz but detected in the correct frequency order of magnitude. The later is probably due to the larger concentration of our sample compared to that examined experimentally. The more accurate results of the present study compared to previous works in the reproduction of $\delta 1$-relaxation we believe are mainly due to the decomposition of the hydration shells combined with good statistics. A more detailed analysis revealed that a portion of water molecules in the first as well in the second hydration shell exhibit dielectric properties similar to those of the bulk.

Moreover, our simulations revealed that a weak and very fast relaxation (here denoted as the ε-process) is present in the first and second solvation shells, which contributes with a peak at ~5×10^{11} Hz in the loss spectrum. Very fast rotations of water molecules, suggested by the ε-process, are possible for water molecules lacking inter-water hydrogen bonding polarized near the protein's surface. In addition, water molecules near polar residues show a somewhat slower relaxation than those near non-polar ones. Polar group bridging water molecules located in the substrate binding cleft as well as those forming a network in internal hydration sites are characterized mainly by a very slow relaxation and less importantly by an ultrafast one. Finally, we were able to calculate the static dielectric constants of the protein, the first and second solvation shells employing two different approaches (i.e., K–F and LRT). Comparison of the results showed that the main discrepancy between the two methods lies in the calculation of the dielectric constant corresponding to the second hydration shell, most probably due to the breakdown of the homogeneity hypothesis in the F–K approach.

Acknowledgments This work has been financially supported partly by the postgraduate courses of the Department of Biochemistry and Biotechnology "Biotechnology—Quality Assessment in Nutrition and the Environment" and "Applications of Molecular Biology- Genetics—Diagnostic Biomarkers". Most simulations of this work have been performed on the HellasGrid infrastructure.

Appendix

As mentioned in section "Theoretical Background" (Eq. 3), the susceptibility χ can be expressed in terms of a Fourier–Laplace transform of the dipole moment time auto- (or cross-) correlation function. In the case of ions it takes the form:

$$\chi_{ij} - \frac{i\sigma(0)}{\omega} = \frac{1}{3Vk_BT} L\left[-\frac{\mathrm{d}}{\mathrm{d}t}\langle \mathbf{M}_\mathrm{I}(0)\cdot\mathbf{M}_\mathrm{I}(t)\rangle\right] - \frac{i\sigma(0)}{\omega} = \frac{i}{3Vk_BT} L[\langle \mathbf{J}_\mathrm{I}(0)\cdot\mathbf{J}_\mathrm{I}(t)\rangle] - \frac{i\sigma(0)}{\omega} \quad (12)$$

where the term of the static conductivity $i\sigma(0)/\omega$ is simply subtracted from both sides, because it is typically eliminated from the experimental spectrum. $\Phi_\mathrm{II}(t) = \langle \mathbf{J}_\mathrm{I}(0)\cdot\mathbf{J}_\mathrm{I}(t)\rangle$ is the time autocorrelation function of the ionic current, which in our case includes also the protein current due to its charge (+8e). That is:

$$\mathbf{J}_\mathrm{I}(t) = \mathbf{J}_\mathrm{II}(t) + \mathbf{J}_\mathrm{PI}(t) = \sum_{i=1}^{N} q_i\mathbf{v}_i + Q\mathbf{v}_\mathrm{MC} \quad (13)$$

Here $\mathbf{v}_i$ is the velocity of ion i, Q is the total charge of protein and $\mathbf{v}_\mathrm{MC}$ the velocity of its center of mass.

The expression for the conductivity of the ionic current can be written as:

$$\sigma(\omega) = \frac{1}{3\varepsilon_0 Vk_BT} L[\langle \mathbf{J}_\mathrm{I}(0)\cdot\mathbf{J}_\mathrm{I}(t)\rangle] \quad (14)$$

Table 6 Fit parameters for the current autocorrelation function $f(t)$

n	A_n [(eÅ/ps)^2]	ω_n (rad/ps)	φ (rad)	τ_n (ps)
1	1451.67	−35.84	2.37	0.03
2	106.86	58.13	1.57	0.10
3	−41.60	4.89	0.00	0.63

As in the case of dipole moment contribution, $\langle \mathbf{J}_\mathrm{I}(0) \cdot \mathbf{J}_\mathrm{I}(t) \rangle$ in the above equation is replaced by a fit function

$$f(t) = \sum_{n=1}^{3} A_n \sin(\omega_n t + \varphi_\mathrm{n}) \exp(-t/\tau_n) \tag{15}$$

with fit parameters reported in Table 6. Figure 9 represents the current autocorrelation function of our system as well as an appropriate fit.

The static value of $\sigma(0)$ is given from:

$$\sigma(0) = \frac{1}{3\varepsilon_0 V k_B T} \lim_{\mathrm{t}\to\infty} \int_0^t \mathbf{J}_\mathrm{I}(0) \cdot \mathbf{J}_\mathrm{I}(\mathrm{t}^{'})\mathrm{d}t^{'} \tag{16}$$

Using Eqs. (12–16), the real and the imaginary parts of the current contribution to the frequency-dependent dielectric constant can be found to be:

$$\mathrm{Re}[\varepsilon_I(\omega)] = \frac{1}{3\varepsilon_0 V k_B T} \sum_{n=1}^{3} \frac{A_n t_n}{2\omega} \left[\frac{t_n(\omega_n+\omega)\sin\phi_n - \cos\phi_n}{1+t_n^2(\omega+\omega_n)^2} - \frac{t_n(\omega_n-\omega)\sin\phi_n - \cos\varphi_n}{1+t_n^2(\omega_n-\omega)^2} \right] \tag{17}$$

$$\mathrm{Im}[\varepsilon_I(\omega)] = \frac{1}{3\varepsilon_0 V k_B T} \sum_{n=1}^{3} \frac{A_n t_n}{2\omega} \left[\frac{\sin\phi_n - t_n(\omega-\omega_n)\cos\phi_n}{1+t_K^2(\omega-\omega_K)^2} + \frac{\sin\phi_n + t_n(\omega+\omega_n)\cos\phi_n}{1+t_n^2(\omega+\omega_n)^2} - \frac{2\sin\phi_n + t_n\omega_n\cos\phi_n}{1+t_n^2\omega_n^2} \right] \tag{18}$$

It should be noted that the above expressions have the form of 0/0 for $\omega \to 0$ and this is the result of subtracting the term $i\sigma(0)/\omega$ (see Eq. 1). Using this, we can write:

$$\lim_{\omega\to 0} \mathrm{Re}[\varepsilon_\mathrm{I}(\omega)] = \frac{1}{3\varepsilon_0 V k_B T} \sum_{n=1}^{3} \frac{A_n t_n}{2} \left[\frac{2t_n \sin\phi_n + 4t_n^2\omega_n\cos\phi_n - 2t_n^3\omega_n^2\sin\phi_n}{(1+t_n^2\omega_n^2)^2} \right] \tag{19}$$

Using fit parameters from Table 6 we simply find $\lim_{\varpi\to 0} \mathrm{Re}[\varepsilon_I(\omega)] = -0.007$. This is a negligible contribution compared to that of the dipole moment (Fig. 3) and consequently is ignored in our calculations.

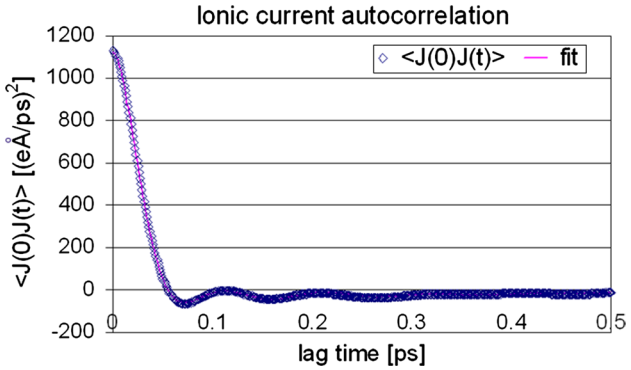

Fig. 9 The autocorrelation function of the current of our system (protein + ions) at 300 K. The *blue diamonds* represent the simulation data, while the *red line* is the corresponding fit

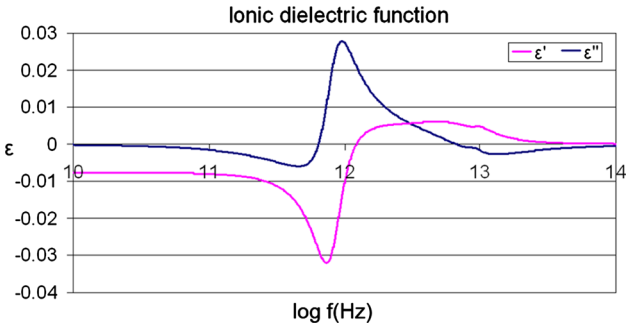

Fig. 10 The ionic contribution (protein + ions) to the real and imaginary part of the frequency-dependent dielectric constant of our system at 300 K

In Fig. 10, the real and the imaginary part of the current contribution to the frequency-dependent dielectric constant is shown.

References

Antosiewicz J, Mccammon J, Gilson M (1994) Prediction of ph-dependent properties of proteins. J Mol Biol 238:415–436

Bonicontro A, Calandrini V, Onori G (2001) Rotational and translational dynamics of lysozyme in water-glycerol solution. Colloid Surf B Biointerfaces 21:311–316

Boresch S, Steinhauser O (1997) Presumed versus real artifacts of the Ewald summation technique: the importance of dielectric boundary conditions. Berichte Der Bunsen-Gesellschaft-Physical Chemistry. Chem Phys 101:1019–1029

Boresch S, Ringhofer S, Hochtl P, Steinhauser O (1999) Towards a better description and understanding of biomolecular solvation. Biophys Chem 78:43–68

Boresch S, Hochtl P, Steinhauser O (2000) Studying the dielectric properties of a protein solution by computer simulation. J Phys Chem B 104:8743–8752

Brooks R, Bruccoleri RE, Olafson BD, States DJ, Swaminathan S, Karplus M (1983) Charmm: a program for macromolecular

energy, minimization and dynamics calculations. Comput Chem 4:187–217
Caillol JM, Levesque D, Weis JJ (1986) Theoretical calculation of ionic solution properties. J Chem Phys 85:6645–6657
Caillol JM, Levesque D, Weis JJ (1989) Electrical properties of polarizable ionic solutions. I. Theoretical aspects. J Chem Phys 91(9):5544–5554
Cametti C, Marchetti S, Gambi C, Onon G (2011) Dielectric relaxation spectroscopy of lysozyme aqueous solutions: analysis of the δ-dispersion and the contribution of the hydration water. J Phys Chem B 115:7144–7153
Darden T, York D, Pedersen L (1993) Particle mesh Ewald: an N log(N) method for Ewald sums in large systems. J Chem Phys 98:10089–10092
Ebbinghaus S, Kim SJ, Heyden M, Yu X, Heugen U, Gruebele M, Leitner DM, Havenith M (2007) An extended dynamical hydration shell around proteins. PNAS 104(52):20749–20752
Fröhlich H (1958) Theory of dielectrics. Oxford University Press, New York
Harvey S, Hoekstra P (1972) Dielectric relaxation spectra of water adsorbed on lysozyme. J Phys Chem 76:2987–2994
Hayashi Y, Shinyashiki N, Yagihara S (2002) Dynamical structure of water around biopolymers investigated by microwave dielectric measurements using time domain reflectometry method. J Non-Cryst Solids 305:328–332
Humphrey W, Dalke A, Schulten K (1996) VMD—visual molecular dynamics. J Mol Gr 14:33–38
Inada Y, Loeffler HH, Rode MB (2002) Librational, vibrational, and exchange motions of water molecules in aqueous Ni(II) solution: classical and QM/MM molecular dynamics simulations. Chem Phys Lett 358(5–6):449–458
Kale L, Skeel R, Bhandarkar M, Brunner R, Gursoy A, Krawetz N, Phillips J, Shinozaki A, Varadarajan K, Schulten K (1999) NAMD2: greater scalability for parallel molecular dynamics. J Comput Phys 151(1):283–312
King G, Lee FS, Warshel A (1991) Microscopic simulations of macroscopic of dielectric constants of solvated proteins. J Chem Phys 95:4366–4377
Kirkwood JG (1939) The dielectric polarization of polar liquids. J Chem Phys 7:911–919
Knocks A, Weingartner H (2001) The dielectric spectrum of ubiquitin in aqueous solution. J Phys Chem 105:3635–3638
Kohler F (1972) The liquid state. Chemie, Weinheim
Loffler G, Schreiber H, Steinhauser O (1997) Calculation of the dielectric properties of a protein and its solvent: theory and a case study. J Mol Biol 270:520–534
Miura N, Asaka N, Shinyashiki N, Mashimo S (1994) Microwave dielectric study on bound water of globule proteins in aqueous solutions. Biopolymers 34:357–364
Nakamura H, Sakamoto T, Wada A (1988) A theoretical study of the dielectric constant of protein. Protein Eng 2:177–183
Nandi N, Bagchi B (1998) Anomalous dielectric relaxation of aqueous protein solutions. J Phys Chem A 102:8217–8221
Neumann M (1986a) Computer simulation and the dielectric constant at finite wavelength. Mol Phys 57:97–121
Neumann M (1986b) Dielectric relaxation in water. Computer simulations with the tip4p potential. J Chem Phys 85:1567–1580
Neumann M, Steinhauser O (1983a) On the calculation of the dielectric constant using the Ewald–Kornfeld tensor. Chem Phys Lett 95:417–422
Neumann M, Steinhauser O (1983b) On the calculation of the frequency-dependent dielectric constant in computer simulations. Chem Phys Lett 102:508–513
Neumann M, Steinhauser O, Pawley GS (1984) Consistent calculation of the static and frequency-dependent dielectric constant in computer simulations. Mol Phys 52:97–113
Oleinikova A, Sasisanker P, Weingärtner H (2004) What can really be learned from dielectric spectroscopy of protein solutions? A case study of ribonuclease A. J Phys Chem B 108(24):8467–8474
Oleinikova A, Smolin N, Brovchenko I (2007) Influence of water clustering on the dynamics of hydration water at the surface of a lysozyme. Biophys J 93:2986–3000
Onsager L (1936) Electric moments of molecules in liquid media. J Am Chem Soc 58:1486–1493
Pethig R (1992) Protein–water interactions determined by dielectric methods. Ann Rev Phys Chem 43:177–205
Rudas T, Schröder C, Boresch S, Steinhauser O (2006) Simulation studies of the protein–water interface. II. Properties at the mesoscopic resolution. J Chem Phys 124(23):234908
Ryckaert JP, Ciccotti G, Berendsen HJC (1977) Numerical integration of the Cartesian equations of motion of a system with constraints: molecular dynamics of n-alkanes. J Comput Phys 23:327–341
Sanner MF, Spenner JC, Olson AJ (1996) Reduced surface: an efficient way to compute molecular surfaces. Biopolymers 38(3):305–320
Simonson T, Perahia D (1995) Internal and interfacial dielectric-properties of cytochrome-c from molecular-dynamics in aqueous-solution. PNAS 92:1082–1086
Simonson T, Perahia D, Brünger AT (1991) Microscopic theory of the dielectric properties of proteins. Biophys J 59:670–690
Smith SW (1999) The scientist and engineer's guide to digital signal processing. Oxford University Press, New York, pp 141–168
Smith PE, Brunne RM, Mark AE, Van Gunsteren WF (1993) Dielectric properties of trypsin inhibitor and lysozyme calculated from molecular dynamics simulations. J Phys Chem 97:2009–2014
Soda K, Shimbo Y, Seki Y, Taiji M (2011) Structural characteristics of hydration sites in lysozyme. Biophys Chem 156:31–42
South G, Grant P (1972) Dielectric dispersion and dipole moment of myoglobin in water. Proc R Soc London Ser A 328:371–387
Suzuki M, Shigematsou J, Kodama T (1996) Hydrophobic hydration analysis on amino acid solutions by the microwave dielectric method. J Phys Chem 100:7279–7282
Svergun DI, Richard S, Koch MHJ, Sayers Z, Kuprin S, Zaccai G (1998) Protein hydration in solution: experimental observation by X-ray and neutron scattering. P Natl Acad Sci USA Biophys 95:2267–2272
Weingärtner H, Knocks A, Boresch S, Hochtl P, Steinhauser O (2001) Dielectric spectroscopy in aqueous solutions of oligosaccharides: experiment meets simulation. J Chem Phys 115:1463–1472
Yang L, Weerasinghe S, Smith P, Pettitt B (1995) Dielectric response of triplex DNA in ionic solution from simulations. Biophys J 69:1519–1527
Yokoyama K, Kamei T, Minami H, Susuki M (2001) Hydration study of globular proteins by microwave dielectric spectroscopy. J Phys Chem 105:12622–12627